

Uncoupling protein 1-driven Cre (*Ucp1-Cre*) is expressed in the epithelial cells of mammary glands and various non-adipose tissues



Kyungchan Kim¹, Jamie Wann¹, Hyeong-Geug Kim¹, Jisun So¹, Evan D. Rosen², Hyun Cheol Roh^{1,*}

ABSTRACT

Objective: Uncoupling protein 1 (UCP1), a mitochondrial protein responsible for nonshivering thermogenesis in adipose tissue, serves as a distinct marker for thermogenic brown and beige adipocytes. *Ucp1-Cre* mice are thus widely used to genetically manipulate these thermogenic adipocytes. However, evidence suggests that UCP1 may also be expressed in non-adipocyte cell types. In this study, we investigated the presence of UCP1 expression in different mouse tissues that have not been previously reported.

Methods: We employed *Ucp1-Cre* mice crossed with Cre-inducible transgenic reporter Nuclear tagging and Translating Ribosome Affinity Purification (NuTRAP) mice to investigate *Ucp1-Cre* expression in various tissues of adult female mice and developing embryos. Tamoxifen-inducible *Ucp1-CreERT2* mice crossed with NuTRAP mice were used to assess active *Ucp1* expression in adult mice. Immunostaining, RNA analysis, and single-cell/nucleus RNA-seq (sc/snRNA-seq) data analysis were performed to determine the expression of endogenous UCP1 and *Ucp1-Cre*-driven reporter expression. We also investigated the impact of UCP1 deficiency on mammary gland development and function using *Ucp1*-knockout (KO) mice.

Results: *Ucp1-Cre* expression was observed in the mammary glands within the inguinal white adipose tissue of female *Ucp1-Cre*; NuTRAP mice. *Ucp1-Cre* was activated during embryonic development in various tissues, including mammary glands, as well as in the brain, kidneys, eyes, and ears, specifically in epithelial cells in these organs. However, *Ucp1-CreERT2* showed no or only partial activation in these tissues of adult mice, indicating the potential for low or transient expression of endogenous *Ucp1*. While sc/snRNA-seq data suggest potential expression of UCP1 in mammary epithelial cells in adult mice and humans, *Ucp1*-KO female mice displayed normal mammary gland development and function.

Conclusions: Our findings reveal widespread *Ucp1-Cre* expression in various non-adipose tissue types, starting during early development. These results highlight the importance of exercising caution when interpreting data and devising experiments involving *Ucp1-Cre* mice.

© 2024 The Author(s). Published by Elsevier GmbH. This is an open access article under the CC BY-NC-ND license (<http://creativecommons.org/licenses/by-nc-nd/4.0/>).

Keywords *Ucp1-Cre*; UCP1; Mammary gland; Epithelial cells; Brown and beige adipocytes; Adipose tissue

1. INTRODUCTION

Adipose tissues play a crucial role in energy balance and metabolic homeostasis. These tissues not only store energy in the form of lipids but also function as an endocrine organ by secreting various hormones and cytokines that regulate energy metabolism and insulin sensitivity [1]. Adipose tissue is broadly classified into two types, white adipose tissue (WAT) and brown adipose tissue (BAT). WAT primarily functions in the role of energy storage, whereas BAT dissipates energy through nonshivering thermogenesis for thermal regulation. While these two adipose tissue types are located in anatomically distinct locations, a third type of adipocyte—the thermogenic beige adipocyte—has been identified to emerge within WAT upon cold exposure [2–4]. These thermogenic brown and beige adipocytes have gained significant

attention due to their potential to counteract obesity and related metabolic disorders [5].

The thermogenic function of brown and beige adipocytes is primarily contributed by mitochondrial uncoupling protein 1 (UCP1) [6]. UCP1 uses the proton gradient across the mitochondrial inner membrane to generate heat by uncoupling oxidative phosphorylation from ATP production. While recent studies have revealed UCP1-independent thermogenic mechanisms [7,8], UCP1 expression remains a hallmark of thermogenic adipocytes. The study of these thermogenic adipocytes has been greatly facilitated by the development of the *Ucp1-Cre* transgenic mouse line [9], allowing for genetic manipulation and labeling of UCP1-expressing thermogenic adipocytes *in vivo*, significantly advancing our understanding of adipose biology.

¹Department of Biochemistry and Molecular Biology, Indiana University School of Medicine, Indianapolis, IN 46202, USA ²Division of Endocrinology, Diabetes and Metabolism, Beth Israel Deaconess Medical Center, Boston, MA 02215, USA

*Corresponding author. 635 Barnhill Drive, MS1021G, Indianapolis, IN 46202, USA. E-mail: hyunroh@iu.edu (H.C. Roh).

Abbreviations: WAT, White adipose tissue; BAT, Brown adipose tissue; UCP1, Uncoupling protein 1; iWAT, Inguinal white adipose tissue; KO, Knockout; sc/snRNA-seq, Single-cell/nucleus RNA-seq; NuTRAP, Nuclear tagging and Translating Ribosome Affinity Purification; E13.5, Embryonic day 13.5; E16.5, Embryonic day 16.5

Received October 7, 2023 • Revision received April 19, 2024 • Accepted April 23, 2024 • Available online 25 April 2024

<https://doi.org/10.1016/j.molmet.2024.101948>

Accumulating studies have documented the expression of UCP1 in various non-adipose tissues, such as the kidneys, adrenal glands, skeletal muscle, heart, thymus, brain, and gastrointestinal tract [10–17]. Although the extent and functional implications of this expression are still under investigation, the presence of UCP1 in these non-adipose tissues suggests potential roles beyond thermogenesis, including metabolic regulation and protection against oxidative stress [11]. Obviously, the expression of UCP1 in non-adipose tissues raises concerns regarding the tissue specificity of *Ucp1-Cre* for generating mouse models with brown/beige adipocyte-specific genetic perturbations. Indeed, Clafin et al. observed the expression of *Ucp1-Cre* not only in adipose tissues but also in other tissues, such as the kidneys, adrenal glands, and hypothalamus [10]. This suggests that there may be potential off-target effects on non-adipose tissues when using *Ucp1-Cre* mice for specific targeting of brown/beige adipocytes. In our study, we report the expression of *Ucp1-Cre* in myoepithelial and ductal epithelial cells of the mammary gland located within the inguinal WAT (iWAT) of female mice. The expression of *Ucp1-Cre* in the mammary glands occurs during embryonic development. *Ucp1-Cre* is also found in epithelial cells in various non-adipose tissues in developing embryos, including the eyes, ears, whisker follicles, and brain. Some of these non-adipose tissues show potential endogenous *Ucp1* expression in adult mice, albeit at low and transient levels. Single-cell and nucleus RNA sequencing (sc/snRNA-seq) data suggest the possibility of UCP1 expression in mammary glands postnatally in mice and humans. Nevertheless, *Ucp1*-knockout (KO) mouse studies suggest that UCP1 is not necessary for the development or function of the mammary glands. Our study highlights that it is crucial to consider the broad expression pattern of *Ucp1-Cre* in studies that employ mouse models utilizing this genetic tool.

2. MATERIAL AND METHODS

2.1. Animals

All animal experiments were performed according to procedures approved by the Beth Israel Deaconess Medical Center (BIDMC) Institutional Animal Care and Use Committee and the Indiana University School of Medicine (IUSM) Institutional Animal Care and Use Committee. To label UCP1-expressing cells, NuTRAP (Nuclear tagging and Translating Ribosome Affinity Purification) mice (Jackson Laboratory, 029899) [18] were crossed with *Ucp1-Cre* mice (Jackson Laboratory, 024670) [9] and *Ucp1-CreERT2* mice [19], respectively. Mice were housed under a 12-hour light/12-hour dark cycle with ad libitum access to a standard chow diet and water at 22 °C for standard room temperature housing. To evaluate the Cre recombinase activity in response to cold and thermoneutrality, mice were housed in 4 °C and 30 °C incubators for 1 week and 4 weeks, respectively. *Ucp1*-KO mice (Jackson Laboratory, 003124) were used for lactation assays.

2.2. Tamoxifen injection

Tamoxifen (Sigma, T5648) was dissolved in sunflower seed oil (Sigma, S5007) at a concentration of 20 mg/mL by incubating at 37 °C overnight with agitation. The mice (6–12 weeks old) were then intraperitoneally injected with tamoxifen at a dosage of 100 mg/kg for three consecutive days. After a washout period of 3 days following the last injection, the mice were euthanized to collect tissue samples. For tamoxifen injection in mice exposed to cold, the animals were incubated at 4 °C for 1 week. Subsequently, while remaining in the cold incubator, the mice were injected with tamoxifen for 3 days and kept for another 3 days for washout until termination.

2.3. Lactation assay

Ucp1-KO or heterozygous female mice were mated with wild-type C57BL/6 male mice, and then body weight measurements of their offspring were taken during the 2-week lactation period. The day immediately after weaning, female breeders were sacrificed for histological analysis of iWAT.

2.4. Immunohistochemistry

Dissected tissues and embryos were fixed in 10% formalin for 1–2 days at 4 °C, washed in PBS, and processed for paraffin-embedded sections by the BIDMC or IUSM histology core. For immunohistochemical staining, sections were deparaffinized and then treated with sodium citrate for antigen retrieval and hydrogen peroxide for endogenous peroxidase inactivation. The sections were subsequently blocked with donkey serum and incubated with rabbit anti-GFP antibody (1:500; Abcam, ab290) or rabbit anti-UCP1 antibody (1:500; Abcam, ab10983) at 4 °C overnight. After extensive washing in PBS with 0.05% Tween-20, the sections were incubated with a horseradish peroxidase-conjugated donkey anti-rabbit secondary antibody (1:3000; Jackson ImmunoResearch, 711-035-152), developed in diaminobenzidine, and counter-stained with hematoxylin.

2.5. Immunofluorescence staining

Mice were anesthetized with an intraperitoneal injection of avertin (300 mg/kg), then transcardially perfused with cold PBS followed by cold 4% paraformaldehyde in PBS. The brain was processed, embedded, and cryosectioned as previously described [20]. Dissected peripheral tissues were fixed in 4% paraformaldehyde in PBS for 1 day at 4 °C and then immersed in 30% sucrose in PBS for 2 days. To prepare frozen sections, the tissues were embedded in an optimal cutting temperature compound (Sakura Finetek, 4583) and frozen on dry ice. Serial sections (10–20 μm) were cut on a cryostat (Leica, CM1950), mounted on adhesive glass slides (Matsunami, SUMGP11), and air dried for 2 h at room temperature. After extensive rinsing in PBS, the sections were blocked in PBS with 5% donkey serum and 0.1% Triton X-100 for 1 h at room temperature and incubated in a mixture of goat anti-GFP (1:300; Novus, nb100-1678) and rabbit anti-UCP1 (1:300; Abcam, ab10983) primary antibodies in the same blocking buffer at 4 °C overnight. After extensive rinsing in PBS with 0.05% Tween-20, Alexa488-conjugated donkey anti-goat (1:300; Invitrogen, A11055) and Alexa568-conjugated donkey anti-rabbit (1:300; Invitrogen, A10042) secondary antibodies were applied for 1 h at room temperature. The sections were subsequently incubated for 10 min with 1 μg/mL Hoechst 33258 (Invitrogen, Thermo Fisher Scientific) in PBS for nuclear staining, then mounted on glass slides, and coverslipped with VECTASHIELD Mounting Medium (Vector Laboratories). Sections were visualized under Leica TCS SP8 confocal laser-scanning microscope.

2.6. RNA extraction and qRT-PCR

TRIzol reagent (Ambion, Thermo Fisher Scientific) and chloroform were used to extract total RNA from each tissue, according to the manufacturer's protocol. cDNA synthesis and qRT-PCR analysis were performed as we have described previously [21]. The primer sequences used for qRT-PCR are as follows: *Ucp1*: Forward-ACTGCCACACCTCCAGTCATT, Reverse-CTTTGCCTCACTCAGGATTGG, *GFP*: Forward-GCGGCGTCCAGAACTC, Reverse-AGCAAAGACCCCAAGAGAA, *36B4*: Forward-GAGGAATCAGATGAGGATATGGGA, Reverse-AAGCAGGCTGACTTGGTTGC.

2.7. Single cell/nucleus RNA-seq (sn/scRNA-seq) analysis

The snRNA-seq data from mouse adipose tissue [22] were accessed and analyzed using the Single Cell Portal provided by the Broad Institute (https://singlecell.broadinstitute.org/single_cell). The human scRNA-seq data [23] were accessed through the Human Protein Atlas [24]. The UCP1 expression data were retrieved directly from the databases without any additional processing.

2.8. Data analysis

Two-tailed unpaired Student's *t* test was carried out using GraphPad Prism 8. Data are presented as mean \pm SEM and significance was determined at $P < 0.05$. GFP imaging and immunostaining analyses were performed with 3–6 sections from each mouse (at least 3 mice), and representative data were presented.

3. RESULTS

3.1. *Ucp1-Cre* is expressed in the mammary glands of female mice

We previously developed a transgenic reporter mouse called NuTRAP. This mouse harbors a transgene cassette at the *Rosa26* locus that produces GFP-tagged ribosomes and mCherry-tagged nuclei. The cassette is preceded by a loxP-flanked stop sequence, enabling transgene expression in a Cre recombinase-dependent manner [18]. This mouse is useful for conducting transcriptional and epigenomic analyses in a cell type-specific manner [25]. As Cre-mediated recombination removes the stop sequence and subsequently leads to permanent labeling of the cells, it can be utilized for lineage tracing studies by tracking GFP/mCherry expression. To investigate UCP1-expressing beige adipocytes, we generated NuTRAP crossed with *Ucp1-Cre* mice and exposed these mice to cold conditions for 1 week. Following immunohistochemical staining of GFP in the male mice subjected to cold temperatures, we observed specific GFP expression in dense multilocular beige adipocytes within the iWAT depot (Figure 1A), which is consistent with our previous study [26]. Interestingly, female *Ucp1-Cre*; NuTRAP mice exhibited GFP expression not only in beige adipocytes but also in cell types within the mammary gland, including myoepithelial and luminal epithelial cells (Figure 1B). The abundance of GFP-expressing beige adipocytes was significantly changed in response to different housing temperatures: highest in the cold, intermediate at room temperature, and lowest under thermo-neutral conditions (Figure 1C). However, GFP-expressing cells in the mammary gland did not exhibit a temperature-dependent response (Figure 1C). When we conducted UCP1 immunohistochemical staining on consecutive iWAT sections from the cold-exposed female *Ucp1-Cre*; NuTRAP mice, we found UCP1 staining in both beige adipocytes and mammary gland cells, similar to the GFP staining (Figure S1A). Nonetheless, there was high background staining (Figure S1A), which raised concerns about the specificity of the UCP1 antibody. To address this issue, we performed UCP1 immunohistochemical staining on iWAT from female *Ucp1-KO* mice. As previously reported [27,28], we observed a higher number of multilocular beige adipocytes in the iWAT of *Ucp1-KO* mice compared to the control *Ucp1* heterozygous mice (Figure S1B). These beige adipocytes in *Ucp1-KO* mice were negative for UCP1 expression. However, UCP1 immunoreactivity was still evident in the mammary glands of both *Ucp1-KO* and heterozygous mice (Figure S1B), suggesting that non-specific activity of the UCP1 antibody may lead to false-positive staining in mammary glands. To determine whether UCP1 is expressed in mammary glands, we employed a different approach using NuTRAP crossed with tamoxifen-inducible *Ucp1-CreERT2* mice, which allows GFP-labeling of cells with active *Ucp1* expression at the time of tamoxifen injection. We exposed

female *Ucp1-CreERT2*; NuTRAP mice to cold temperatures for 1 week and administered tamoxifen for three consecutive days during cold exposure. Immunohistochemical staining using a GFP antibody revealed that GFP was expressed exclusively in beige adipocytes but not in the mammary glands within the iWAT of *Ucp1-CreERT2*; NuTRAP mice (Figure 1D). Immunofluorescence co-staining showed that most beige adipocytes were positive for both UCP1 and GFP (Figure S1C). In contrast, mammary gland cells were only positive for UCP1, likely due to non-specific staining (Figure S1C). These results indicate that UCP1 is not actively expressed in the mammary glands of adult female mice. Instead, they suggest the possibility that *Ucp1-Cre* may have been once activated in mammary epithelial cell lineages during earlier development, indicating a history of the *Ucp1* expression.

3.2. *Ucp1-Cre* expression is initiated in multiple tissues during embryonic development

To determine when *Ucp1-Cre* becomes active in the mammary glands during development, we examined GFP expression in developing *Ucp1-Cre*; NuTRAP embryos. Through gross visual inspection of developing mouse embryos, we identified green fluorescence in the mammary epithelial buds on embryonic day 13.5 (E13.5) (Figure 2A and B). We also found green fluorescence in other areas, including the brain, eyes, whisker follicles, and internal organs (Figure 2A and C). Subsequently, to confirm GFP expression, we performed immunohistochemical staining for GFP on sagittal or cross sections of the E13.5 embryos. We observed GFP expression in the epithelial layer of the choroid plexus in the forebrain (lateral ventricles) and hindbrain (fourth ventricles) (Figure 2D), renal tubular epithelial cells in the kidney (Figure 2E), scleral cells in the eye (Figure 2F), and the epithelium of the sacculle, utricle, and semicircular ducts in the inner ear (Figure 2G). Interestingly, GFP expression was not yet detected in the developing BAT even at a later developmental stage of E16.5 (Figure 2H). UCP1 immunohistochemical staining failed to reveal any specific signals apart from high non-specific background signals throughout the entire E13.5 embryo sections (Figure S2). These results suggest that a history of *Ucp1-Cre* activation can be observed in various types of tissues, including the brain, kidneys, eyes, and ears, during embryonic development.

3.3. Endogenous *Ucp1* is potentially expressed in non-adipose tissues in adult mice

To determine whether UCP1 is actively expressed in these non-adipose tissues in adult mice, we analyzed the mRNA expression of *Ucp1* and *GFP* in various tissues from both male and female *Ucp1-CreERT2*; NuTRAP mice housed at room temperature. We examined the kidney (cortex and medulla) and hypothalamus, where we and others observed *Ucp1-Cre* expression [10], along with the *Ucp1-Cre*-negative liver. As positive controls for *Ucp1* expression, we included BAT and iWAT. In both male and female mice, BAT and iWAT exhibited high levels of *Ucp1* expression in both Cre-negative NuTRAP and *Ucp1-CreERT2*; NuTRAP mice (Figures S3A and S3C). *GFP* expression was strongly induced specifically in *Ucp1-CreERT2*; NuTRAP mice of both sexes (Figures S3B and S3D). In contrast, we detected very low levels of *Ucp1* in the kidney, hypothalamus, and liver, and *GFP* expression was not induced in these tissues from *Ucp1-CreERT2*; NuTRAP mice of either sex (Figure S3). Similar results were obtained in the tissues from female *Ucp1-CreERT2*; NuTRAP mice exposed to cold temperatures (Figure S4).

To precisely assess GFP expression driven by the *Ucp1* promoter, we visualized GFP fluorescence in various tissue sections from *Ucp1-CreERT2*; NuTRAP and *Ucp1-Cre*; NuTRAP mice. In adipose tissues,

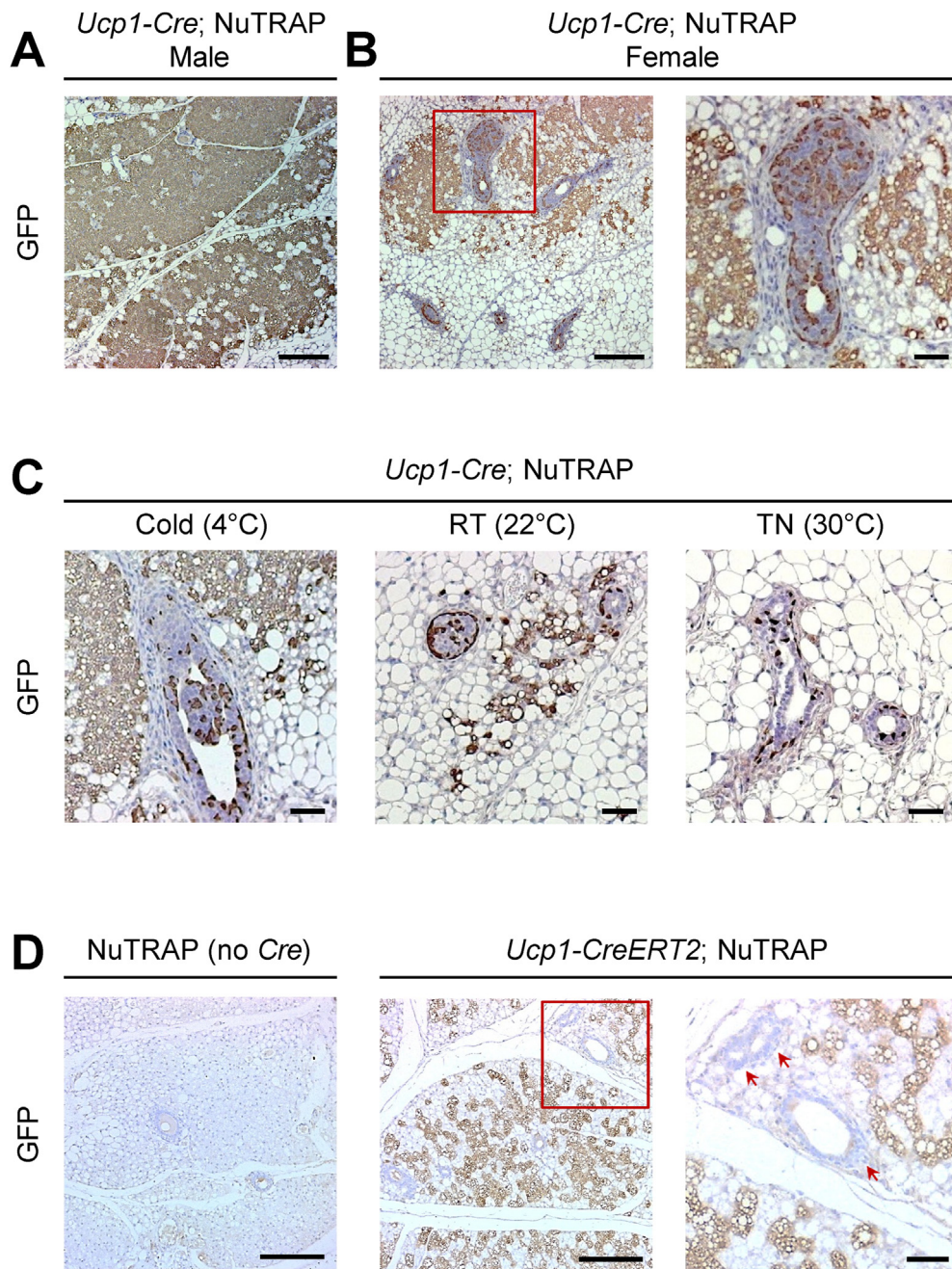


Figure 1: *Ucp1-Cre* expression but not endogenous *Ucp1* in the mammary glands of female mice. Immunohistochemical staining for GFP in iWAT depots. (A) Male *Ucp1-Cre; NuTRAP* mouse exposed to cold conditions (4 °C, 1 week). Scale bars, 200 μm. (B) Female *Ucp1-Cre; NuTRAP* mouse exposed to cold. Magnified inset shown on the right. Scale bars, 200 μm and 50 μm (inset). (C) Female *Ucp1-Cre; NuTRAP* mice under cold (4 °C, 1 week), room temperature (RT; 22 °C), and thermoneutrality (TN; 30 °C, 4 weeks) conditions. Scale bars, 50 μm. (D) Female NuTRAP (Cre-negative control) and *Ucp1-CreERT2; NuTRAP* mice after tamoxifen injection during 1-week cold exposure. Magnified inset shown on the right. Red arrows indicate mammary glands. Scale bars, 200 μm and 50 μm (inset).

GFP expression was observed as expected (Figure S5). In both *Ucp1-CreERT2; NuTRAP* and *Ucp1-Cre; NuTRAP* mice, regardless of sex, nearly all adipocytes in BAT were GFP-positive. Notably, GFP expression in *Ucp1-CreERT2; NuTRAP* mice was relatively heterogeneous and weaker, potentially due to the effects of tamoxifen injection. In epididymal WAT, GFP was not detected in any of the mouse lines or sexes. In iWAT, GFP expression was observed in a subset of adipocytes in both mouse lines, regardless of sex. However, GFP expression in the mammary gland was only found in female *Ucp1-Cre; NuTRAP* mice

(Figure S5B), consistent with the aforementioned results. We examined the adrenal glands, thymus, liver, and pancreas, all of which were negative for GFP (Figure S6). In the adrenal glands, we observed significant autofluorescence within the tissues, while GFP expression was indeed detected only in the adjacent adipose tissues (Figure S6). As in embryos, we observed significant GFP expression in the kidneys of adult *Ucp1-Cre; NuTRAP* mice, with the highest expression in the papilla, and progressively less in the medulla and cortex (Figure 3A and B). In contrast, *Ucp1-CreERT2; NuTRAP* mice exhibited no GFP

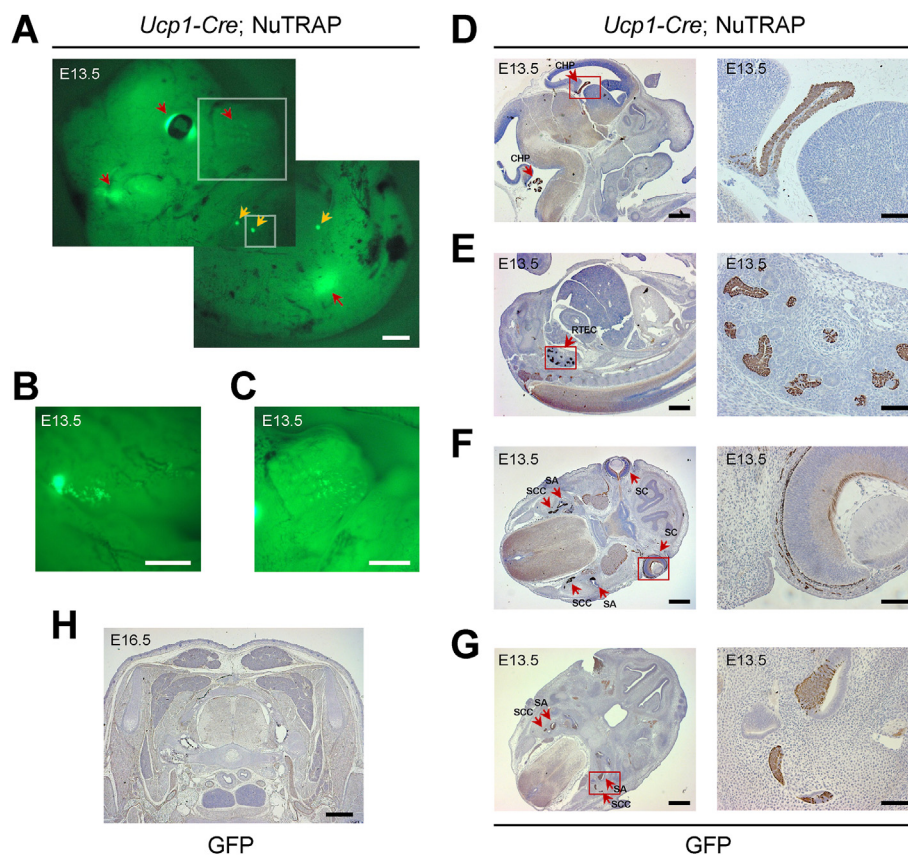


Figure 2: *Ucp1-Cre* activation in multiple tissues during embryonic development. (A–C) GFP fluorescence in *Ucp1-Cre*; NuTRAP embryo on embryonic day 13.5 (E13.5). The entire embryo (A), magnified insets for the mammary gland (B) and whisker follicles (C) are shown. Orange arrows indicate GFP expression in the developing mammary glands. Red arrows indicate GFP expression in the brain, eyes, whisker follicles, and internal organs. Scale bars, 500 μ m (A and B) and 200 μ m (C). (D–H) Immunohistochemical staining for GFP in *Ucp1-Cre*; NuTRAP embryos. Magnified insets are shown on the right. (D) Sagittal sections showing the choroid plexus (CHP) in the brain. (E) Sagittal sections showing renal tubular epithelial cells (RETC). (F and G) Cross sections showing scleral cells (SC), saccule/utricle (SA), and semi-circular canal (SCC). (H) Cross sections showing the brown adipose tissues. Note: no GFP expression detected. Scale bars, 500 μ m and 50 μ m (insets).

expression in the renal cortex and medulla, but we did observe weak, albeit significant, GFP expression in the papilla (Figure 3A and B). Consistently, we also detected significant *GFP* mRNA expression in the renal papilla of *Ucp1-CreERT2*; NuTRAP mice (Figure S7). In the brain of *Ucp1-Cre*; NuTRAP mice, GFP expression was identified in various regions, with the strongest in the choroid plexus, followed by the parafascicular thalamic nucleus, amygdala, and hypothalamus (Figure 3C and D). Although substantially weaker and in a smaller number of cells, GFP expression was also detected in the brain of *Ucp1-CreERT2*; NuTRAP mice. GFP was frequently observed in the choroid plexus and parafascicular thalamic nucleus, less commonly in the amygdala, and no GFP-positive cells were found in any hypothalamic regions, including the ventromedial hypothalamus (Figure 3C and D). These results were consistent across both male and female mice. These findings indicate that the *Ucp1* promoter is active in specific central and peripheral non-adipose tissues of adult mice, though the activity is at low levels or transient, suggesting the potential expression of endogenous *Ucp1* in these tissues.

3.4. sn/scRNA-seq data suggest potential endogenous UCP1 expression in mammary glands

To investigate the expression of endogenous UCP1, we utilized publicly available sn/scRNA-seq databases. Our analysis of the snRNA-seq data obtained from adult mouse WATs [22], including both iWAT and

perigonadal WAT from both males and females, demonstrated prominent *Ucp1* expression in adipocyte populations (Figure S8A–S8C). Furthermore, we observed *Ucp1* expression, albeit in very low cell numbers, in the female epithelial cells (Figure S8C), which are myoepithelial cells of mammary glands. Of note, *Ucp1* expression was also detected in other cell types, such as macrophages, male epithelial cells, and mesothelial cells (Figure S8C). We subsequently extended our investigation to human tissues by analyzing scRNA-seq data available from the Human Protein Atlas [23]. Consistent with the mouse data, *UCP1* expression was detected in breast glandular and myoepithelial cells in humans (Figure S8D). These findings suggest the possibility of endogenous UCP1 expression in mammary glands in adults.

3.5. UCP1 deficiency has no impact on mammary gland structure or functions

Given the potential expression of UCP1 in myoepithelial and luminal cells in the mammary glands, we sought to investigate whether UCP1 is involved in mammary gland development and function. We first examined the structure of mammary glands in female UCP1-deficient mice, both non-pregnant and lactating post-delivery. In both cases, *Ucp1*-KO female mice exhibited abundant multilocular beige adipocytes in iWAT (Figure 4A), as previously reported [27,28]. However, the structure of the mammary glands, including the

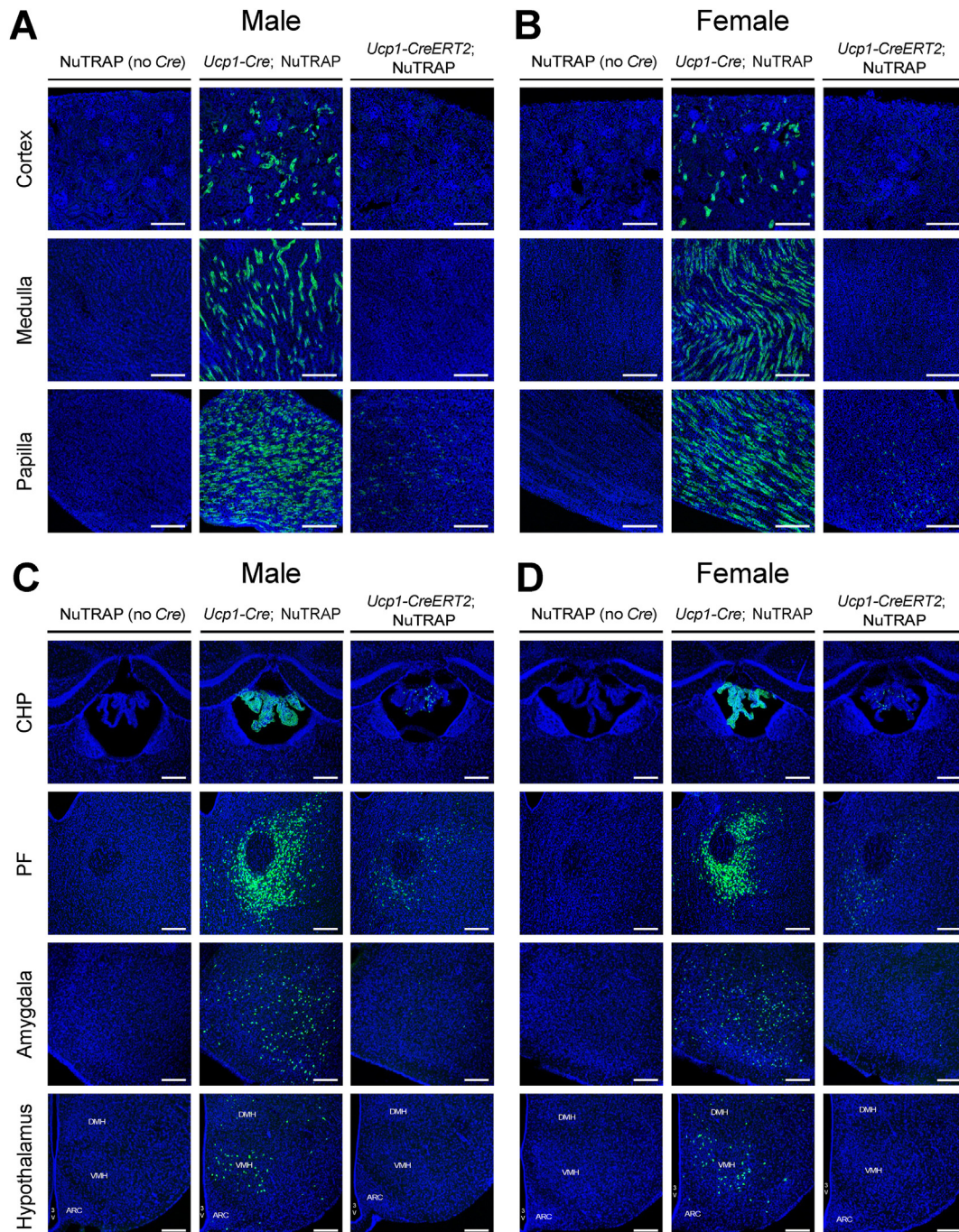


Figure 3: *Ucp1* expression in the kidney and brain of adult mice. (A and B) GFP fluorescence in the kidney of NuTRAP (Cre-negative control), *Ucp1-Cre*; NuTRAP, and *Ucp1-CreERT2*; NuTRAP mice. The panels show the cortex (top), medulla (middle), and papilla (bottom) in male (A) and female (B) mice. (C and D) GFP fluorescence in the brain, showing the choroid plexus (CHP), parafascicular thalamic nucleus (PF), amygdala, and hypothalamus in each row, for male (C) and female (D) mice. Specific areas in the hypothalamus are labeled: 3V, third ventricle; DMH, dorsomedial hypothalamic nucleus; VMH, ventromedial hypothalamic nucleus; ARC, arcuate nucleus. Scale bars, 200 μ m.

morphology of ductal and alveolar regions, appeared similar between *Ucp1*-KO and control heterozygous mice, regardless of whether they were in a non-pregnant or lactating state (Figure 4A). To assess the functionality of the mammary glands, we crossed *Ucp1*-KO or heterozygous female mice with wild-type male mice and monitored the body weight of the resulting pups during a two-week lactation period. *Ucp1* heterozygous female mice served as better

controls than wild-type female mice when crossed with wild-type male mice since 50% of their pups shared the same genotypes as those from *Ucp1*-KO mothers. This approach minimized the effects of genotype differences in the pups. There was no significant difference in the body weights of the pups between the different maternal genotypes (Figure 4B), indicating a similar nutritional content from lactation and comparable functionality of the mammary

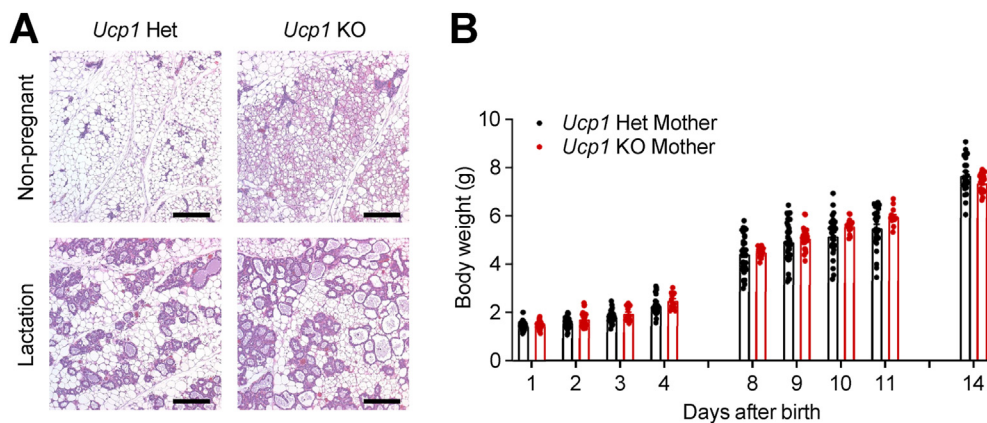


Figure 4: Normal development and function mammary glands in *Ucp1*-deficient mouse. (A) H&E staining of iWAT sections from *Ucp1* heterozygous (Het) and KO mice under non-pregnant (top) and lactation states (bottom). Scale bars, 200 μ m. (B) Body weights of pups born to lactating female mice with *Ucp1* Het ($n = 7$ mothers, 27 pups) or KO ($n = 4$ mothers, 18 pups) for 2 weeks after birth. These female mice were mated with wild-type male mice.

glands between genotypes. Taken together, these results suggest that the loss of UCP1 may not have a significant impact on mammary gland development and function.

4. DISCUSSION

UCP1 is widely recognized as one of the marker genes exclusively expressed in brown and beige adipocytes. *Ucp1-Cre* mice have been a crucial tool for studying thermogenic adipocytes, particularly for generating a variety of mouse models with specific genetic perturbations in brown and beige adipocytes. However, the utility of *Ucp1-Cre* mice has recently been questioned due to the finding of Cre activity in additional tissues, including the kidneys, adrenal glands, and hypothalamus, all of which contribute to energy homeostasis [10]. Therefore, it is important to carefully investigate *Ucp1-Cre* expression and exercise caution when interpreting findings from studies using this model.

In this study, using *Ucp1-Cre*-driven NuTRAP reporter mice, we found a history of *Ucp1-Cre* expression in myoepithelial and luminal cell layers within the mammary glands of female mice. This suggests the possibility of endogenous UCP1 expression in cell types other than adipocytes within adipose tissues. This expression in the mammary gland remained unaffected by changes in ambient temperature, unlike the cold-inducibility of *Ucp1* in adipocytes. Our initial UCP1 immunostaining analysis indicated the presence of UCP1 in mammary glands. However, the subsequent experiments using *Ucp1-KO* mice suggested that UCP1 staining in mammary glands was likely a false positive due to the non-specific immunoreactivity of the UCP1 antibody. Furthermore, the failure to induce GFP expression in the mammary glands of tamoxifen-inducible *Ucp1-CreERT2*; NuTRAP mice supported the lack of active UCP1 expression. These results prompted us to investigate the timing of *Ucp1-Cre* expression during development. We found that *Ucp1-Cre* becomes active in the developing mammary buds by E13.5, suggesting that the UCP1 expression may be an early developmental event. Interestingly, when examining sc/snRNA-seq data from both adult mouse and human tissues, we found low-level UCP1 expression in a small number of cells from the mammary glands. This suggests the possibility that UCP1 may be transiently expressed at low levels in adult mammary glands. However, it is also plausible that *Ucp1*-expressing mammary gland cells in the sc/snRNA-seq data represent doublets between *Ucp1*-positive adipocytes and *Ucp1*-negative

mammary gland cells. Given that *Ucp1* was similarly detected in other cell types, such as macrophages, male epithelial cells, and mesothelial cells, these data do not provide definitive conclusions regarding endogenous UCP1 expression. In addition, although UCP1-expressing adipocytes have been demonstrated to impact mammary epithelium differentiation [29], *Ucp1-KO* mice exhibited normal mammary gland development and functionality. As such, it remains an unanswered question whether UCP1 is expressed in and functionally important for adult mammary glands.

Previous studies documented the existence of a specific type of adipocyte known as pink adipocytes, which were proposed to interconvert between mammary gland epithelial cells and subcutaneous adipocytes [30,31]. However, a recent cell tracing study has challenged this notion and provided evidence against adipocyte-to-epithelial cell conversion [32]. Nonetheless, it is possible that UCP1-expressing epithelial cells within the mammary gland are related to the proposed pink adipocytes. In this scenario, rather than pink adipocytes capable of converting into epithelial cells, these UCP1-expressing cells likely represent a committed cell type akin to myoepithelial and ductal cells. Although no functional defects were observed in the mammary glands of *Ucp1-KO* mice, more precise assays for assessing mammary gland functionality, such as oxytocin-induced milk ejection [33], would be necessary to determine the functional significance of UCP1.

A recent study by Patel et al. discovered that mammary luminal epithelial cells produce paracrine secretory factors, named mammo-kines, such as lipocalin 2, which inhibit UCP1 expression in adipocytes within the iWAT of female mice [34]. This study raises some intriguing questions. Are the mammary epithelial cells expressing *Ucp1-Cre* the same as or functioning with those that secrete mammo-kines? Could mammo-kines switch off UCP1 expression in mammary ducts by acting as autocrine factors? Such a mechanism might explain the lack of UCP1 expression in these cells in adult female mice. Further investigation is warranted to determine whether UCP1 expression in mammary gland development plays a role in iWAT homeostasis in female mice.

We observed *Ucp1-Cre* expression in various non-adipose tissues, including previously unreported ones, such as the eyes, ears, and whisker follicles. While *Ucp1-Cre* was activated in these tissues during embryonic development, no apparent developmental defects have been identified in *Ucp1-KO* mice. However, it is worth noting that *Ucp1-KO*

Brief Communication

(*Ucp1^{tm1b(EUCOMM)HmgU}*) mice, produced by the European Conditional Mouse Mutagenesis Program, exhibit eye phenotypes, including abnormal lens morphology and cataract, albeit with low penetrance [35]. These findings suggest that UCP1 might play a role in developmental processes, indicating the necessity for a more thorough investigation. We also found evidence of potential expression of endogenous *Ucp1* in some of these tissues in adult mice. In adult *Ucp1-CreERT2*; NuTRAP mice, we detected GFP expression in the specific kidney and brain regions, indicating active *Ucp1* promoter activity in these tissues at the time of tamoxifen injection in adulthood. The intensity of GFP expression in *Ucp1-CreERT2*; NuTRAP mice was weaker than in *Ucp1-Cre*; NuTRAP mice, but the patterns were consistent across the mouse lines. The papilla in the kidney and the choroid plexus and parafascicular thalamic nucleus in the brain, which showed intense GFP expression in *Ucp1-Cre*; NuTRAP mice, also displayed GFP expression in *Ucp1-CreERT2*; NuTRAP mice. The cortex and medulla in the kidney and the amygdala and hypothalamus in the brain, which showed modest GFP expression in *Ucp1-Cre*; NuTRAP mice, exhibited no or very weak GFP expression in *Ucp1-CreERT2*; NuTRAP mice. Given that *Ucp1-Cre* and *Ucp1-CreERT2* are independently derived bacterial artificial chromosome transgenic lines [9,19], these consistent GFP expression patterns likely reflect genuine *Ucp1* promoter activity in various non-adipose tissues rather than the artifacts arising from the integration sites. The activity of the *Ucp1* promoter appears to be low and/or transient, resulting in significantly lower activation of reporters driven by *Ucp1-CreERT2* compared to those driven by *Ucp1-Cre*. Our findings are in line with the previous study that reported active *Ucp1-Cre* in several regions of the adult mouse brain [10]. While these results suggest the expression of endogenous *Ucp1* in these tissues, we cannot completely exclude technical artifacts due to the bacterial artificial chromosome constructs without directly examining endogenous *Ucp1*. More sensitive methods, such as single-molecule fluorescence *in situ* hybridization, would provide more detailed and conclusive information on endogenous *Ucp1* expression in various tissues. All these data suggest that UCP1 may have different functions in non-adipose tissues that require only a low abundance, unlike its role in adipose thermogenesis, where higher expression is essential. Potential functions in non-adipose tissues may include responses to reactive oxygen species and regulation of cell death [11,36]. In conclusion, our findings reveal that the expression pattern of UCP1 is wider and more dynamic than previously understood. Consequently, it is essential to exercise caution when interpreting data and designing experiments using *Ucp1-Cre* and *Ucp1-CreERT2* mice. Furthermore, the utilization of additional complementary tools, such as adipocyte-specific *Adipoq-Cre* system, should receive thorough consideration during experimental design.

FUNDING

This study was supported by IUSM Showalter Research Trust Fund, IUSM Center for Diabetes and Metabolic Diseases Pilot and Feasibility grant, National Institute of Diabetes and Digestive and Kidney Diseases (R01DK129289), and American Diabetes Association Junior Faculty Award (7-21-JDF-056) to H.C.R.

CREDIT AUTHORSHIP CONTRIBUTION STATEMENT

Kyungchan Kim: Writing — review & editing, Writing — original draft, Visualization, Validation, Methodology, Investigation, Formal analysis, Conceptualization. **Jamie Wann:** Writing — review & editing, Validation, Investigation. **Hyeong-Geug Kim:** Validation, Resources,

Investigation. **Jisun So:** Writing — review & editing, Formal analysis. **Evan D. Rosen:** Writing — review & editing, Resources, Formal analysis. **Hyun Cheol Roh:** Writing — review & editing, Writing — original draft, Visualization, Validation, Supervision, Project administration, Methodology, Investigation, Funding acquisition, Formal analysis, Data curation, Conceptualization.

ACKNOWLEDGEMENTS

We thank Christian Wolfrum for providing *Ucp1-CreERT2* mice. We are grateful for the support from the Histology Core at Beth Israel Deaconess Medical Center and Indiana University School of Medicine.

DECLARATION OF COMPETING INTEREST

None.

DATA AVAILABILITY

Data will be made available on request.

APPENDIX A. SUPPLEMENTARY DATA

Supplementary data to this article can be found online at <https://doi.org/10.1016/j.molmet.2024.101948>.

REFERENCES

- [1] Luo L, Liu M. Adipose tissue in control of metabolism. *J Endocrinol* 2016;231(3):R77–99.
- [2] Young P, Arch JR, Ashwell M. Brown adipose tissue in the parametrial fat pad of the mouse. *FEBS Lett* 1984;167(1):10–4.
- [3] Loncar D. Convertible adipose tissue in mice. *Cell Tissue Res* 1991;266(1):149–61.
- [4] Cousin B, Cinti S, Morroni M, Raimbault S, Ricquier D, Penicaud L, et al. Occurrence of brown adipocytes in rat white adipose tissue: molecular and morphological characterization. *J Cell Sci* 1992;103(Pt 4):931–42.
- [5] Cheng L, Wang J, Dai H, Duan Y, An Y, Shi L, et al. Brown and beige adipose tissue: a novel therapeutic strategy for obesity and type 2 diabetes mellitus. *Adipocyte* 2021;10(1):48–65.
- [6] Harms M, Seale P. Brown and beige fat: development, function and therapeutic potential. *Nat Med* 2013;19(10):1252–63.
- [7] Kazak L, Chouchani ET, Jedrychowski MP, Erickson BK, Shinoda K, Cohen P, et al. A creatine-driven substrate cycle enhances energy expenditure and thermogenesis in beige fat. *Cell* 2015;163(3):643–55.
- [8] Ikeda K, Kang Q, Yoneshiro T, Camporez JP, Maki H, Homma M, et al. UCP1-independent signaling involving SERCA2b-mediated calcium cycling regulates beige fat thermogenesis and systemic glucose homeostasis. *Nat Med* 2017;23(12):1454–65.
- [9] Kong X, Banks A, Liu T, Kazak L, Rao RR, Cohen P, et al. IRF4 is a key thermogenic transcriptional partner of PGC-1alpha. *Cell* 2014;158(1):69–83.
- [10] Clafin KE, Flippo KH, Sullivan AI, Naber MC, Zhou B, Neff TJ, et al. Conditional gene targeting using UCP1-Cre mice directly targets the central nervous system beyond thermogenic adipose tissues. *Mol Metabol* 2022;55:101405.
- [11] Jia P, Wu X, Pan T, Xu S, Hu J, Ding X. Uncoupling protein 1 inhibits mitochondrial reactive oxygen species generation and alleviates acute kidney injury. *EBioMedicine* 2019;49:331–40.
- [12] Frontini A, Rousset S, Cassard-Douclier AM, Zingaretti C, Ricquier D, Cinti S. Thymus uncoupling protein 1 is exclusive to typical brown adipocytes and is not found in thymocytes. *J Histochem Cytochem* 2007;55(2):183–9.

- [13] Wang H, Willershauser M, Karlas A, Gorpas D, Reber J, Ntziachristos V, et al. A dual Ucp1 reporter mouse model for imaging and quantitation of brown and brite fat recruitment. *Mol Metabol* 2019;20:14–27.
- [14] Laursen WJ, Mastrotto M, Pesta D, Funk OH, Goodman JB, Merriman DK, et al. Neuronal UCP1 expression suggests a mechanism for local thermogenesis during hibernation. *Proc Natl Acad Sci U S A* 2015;112(5):1607–12.
- [15] Jastroch M, Buckingham JA, Helwig M, Klingenspor M, Brand MD. Functional characterisation of UCP1 in the common carp: uncoupling activity in liver mitochondria and cold-induced expression in the brain. *J Comp Physiol B* 2007;177(7):743–52.
- [16] Lengacher S, Magistretti PJ, Pellerin L. Quantitative rt-PCR analysis of uncoupling protein isoforms in mouse brain cortex: methodological optimization and comparison of expression with brown adipose tissue and skeletal muscle. *J Cerebr Blood Flow Metabol* 2004;24(7):780–8.
- [17] Nibbelink M, Moulin K, Arnaud E, Duval C, Penicaud L, Casteilla L. Brown fat UCP1 is specifically expressed in uterine longitudinal smooth muscle cells. *J Biol Chem* 2001;276(50):47291–5.
- [18] Roh HC, Tsai LT, Lyubetskaya A, Tenen D, Kumari M, Rosen ED. Simultaneous transcriptional and epigenomic profiling from specific cell types within heterogeneous tissues in vivo. *Cell Rep* 2017;18(4):1048–61.
- [19] Rosenwald M, Perdikari A, Rulicke T, Wolfrum C. Bi-directional interconversion of brite and white adipocytes. *Nat Cell Biol* 2013;15(6):659–67.
- [20] Lee J, Kim K, Cho JH, Bae JY, O'Leary TP, Johnson JD, et al. Insulin synthesized in the paraventricular nucleus of the hypothalamus regulates pituitary growth hormone production. *JCI Insight* 2020;5(16).
- [21] So J, Taleb S, Wann J, Strobel O, Kim K, Roh HC. Chronic cAMP activation induces adipocyte browning through discordant biphasic remodeling of transcriptome and chromatin accessibility. *Mol Metabol* 2022;66:101619.
- [22] Emont MP, Jacobs C, Essene AL, Pant D, Tenen D, Colletuori G, et al. A single-cell atlas of human and mouse white adipose tissue. *Nature* 2022;603(7903):926–33.
- [23] Karlsson M, Zhang C, Mear L, Zhong W, Digre A, Katona B, et al. A single-cell type transcriptomics map of human tissues. *Sci Adv* 2021;7(31).
- [24] The human protein atlas. Available online: <https://www.proteinatlas.org>. [Accessed 27 October 2023].
- [25] Kim K, Taleb S, So J, Wann J, Cheol Roh H. Adipocyte-specific ATAC-seq with adipose tissues using fluorescence-activated nucleus sorting. *J Vis Exp* 2023;193.
- [26] Roh HC, Tsai LTY, Shao M, Tenen D, Shen Y, Kumari M, et al. Warming induces significant reprogramming of beige, but not Brown, adipocyte cellular identity. *Cell Metabol* 2018;27(5):1121–1137 e1125.
- [27] Keipert S, Kutschke M, Lamp D, Brachthäuser L, Neff F, Meyer CW, et al. Genetic disruption of uncoupling protein 1 in mice renders brown adipose tissue a significant source of FGF21 secretion. *Mol Metabol* 2015;4(7):537–42.
- [28] Keipert S, Lutter D, Schroeder BO, Brandt D, Stahlman M, Schwarzmayr T, et al. Endogenous FGF21-signaling controls paradoxical obesity resistance of UCP1-deficient mice. *Nat Commun* 2020;11(1):624.
- [29] Gouon-Evans V, Pollard JW. Unexpected deposition of brown fat in mammary gland during postnatal development. *Mol Endocrinol* 2002;16(11):2618–27.
- [30] Cinti S. Pink adipocytes. *Trends Endocrinol Metabol* 2018;29(9):651–66.
- [31] Giordano A, Smorlesi A, Frontini A, Barbatelli G, Cinti S. White, brown and pink adipocytes: the extraordinary plasticity of the adipose organ. *Eur J Endocrinol* 2014;170(5):R159–71.
- [32] Joshi PA, Waterhouse PD, Kasaian K, Fang H, Gulyaeva O, Sul HS, et al. PDGFR α (+) stromal adipocyte progenitors transition into epithelial cells during lobulo-alveologenesis in the murine mammary gland. *Nat Commun* 2019;10(1):1760.
- [33] Kamikawa A, Seko J. Physiological and pharmacological evaluation of oxytocin-induced milk ejection in mice. *Exp Anim* 2020;69(3):345–53.
- [34] Patel S, Sparman NZR, Arneson D, Alvarsson A, Santos LC, Duesman SJ, et al. Mammary duct luminal epithelium controls adipocyte thermogenic programme. *Nature* 2023;620(7972):192–9.
- [35] International mouse phenotyping consortium. Available online: <https://www.mousephenotype.org/data/genes/MGI:98894>. [Accessed 24 March 2024].
- [36] Demine S, Renard P, Arnould T. Mitochondrial uncoupling: a key controller of biological processes in physiology and Diseases. *Cells* 2019;8(8).